Lab on a Chip

Amplification-Free, Sequence-Specific 16S rRNA Detection at 1 aM

Journal:	*Lab on a Chip*
Manuscript ID	LC-ART-05-2018-000452.R1
Article Type:	Paper
Date Submitted by the Author:	06-Jun-2018
Complete List of Authors:	Koo, Bonhye; UCLA, Chemical and Biomolecular Engineering Yorita, Allison; UCLA, Chemical and Biomolecular Engineering Department Schmidt, Jacob; UCLA, Department of Bioengineering Monbouquette, Harold; University of California, Los Angeles, Chemical and Biomolecular Engineering

Lab on a Chip

Paper

Amplification-Free, Sequence-Specific 16S rRNA Detection at 1 aM†

Received 00th May 2018,
Accepted 00th January 2018

DOI: 10.1039/x0xx00000x

www.rsc.org/

Bonhye Koo[a], Allison M. Yorita[a], Jacob J. Schmidt[b], and Harold G. Monbouquette*[a]

A nucleic acid amplification-free, optics-free platform has been demonstrated for sequence-specific detection of *Escherichia coli* (*E. coli)* 16S rRNA at 1 aM (10^{-18} M) against a 10^6-fold (1 pM) background of *Pseudomonas putida* (*P. putida*) RNA. This work was driven by the need for simple, rapid, and low cost means for species-specific bacterial detection at low concentration. Our simple, conductometric sensing device functioned by detecting blockage of a nanopore fabricated in a sub-micron-thick glass membrane. Upon sequence-specific binding of target 16S rRNA, otherwise charge-neutral, PNA oligonucleotide probe-polystyrene bead conjugates become electrophoretically mobile and are driven to the glass nanopore of lesser diameter, which is blocked, thereby generating a large, sustained and readily observable step decrease in ionic current. No false positive signals were observed with *P. putida* RNA when this device was configured to detect *E. coli* 16S rRNA. Also, when a universal PNA probe complementary to the 16S rRNA of both *E. coli* and *P. putida* was conjugated to beads, a positive response to rRNA of both bacterial species was observed. Finally, the device readily detected *E. coli* at 10 CFU/mL in a 1 mL sample, also against a million-fold background of viable *P. putida*. These results suggest that this new device may serve as the basis for small, portable, low power, and low-cost systems for rapid detection of specific bacterial species in clinical samples, food, and water.

Introduction

New methods for rapid, sensitive, and cost-effective detection of nucleic acids (NAs) of specific sequence are in high demand for a variety of applications including pathogenic disease diagnosis, detection of food contaminants, patient screening during epidemics, and oncological status assessment during surgery. Lack of effective means for infectious disease diagnosis currently contributes to 95% of deaths in developing countries[1] and is an ongoing challenge in developed countries as well. Thus, there is strong impetus for development of inexpensive, robust, fast, and sensitive point-of-care (POC) molecular diagnostic devices for pathogens in clinical samples in particular.

Most existing NA detection methods rely on polymerase chain reaction (PCR) with fluorescence detection of the amplicon.[2, 3] However, all devices reliant on NA amplification require primers, polymerase, nucleotides, and tightly controlled reaction conditions that contribute to complexity and cost. Also, fluorescence detection methods require the incorporation of additional reagents and optics, which adds yet more cost and bulk thereby making a more affordable and portable device harder to achieve. An ideal POC molecular diagnostic device for NA detection therefore would not entail NA amplification or optics.

Over the past 10 years or so, remarkable progress has been made in developing new approaches for amplification-free NA detection at clinically relevant concentrations in the single-digit attomolar (aM, 10^{-18} M) range and below.[4-25] However, only a handful of these schemes do not require special labels other than an oligonucleotide complementary to the target NA.[4, 14-16, 19, 21] Also, nearly half require optics of some kind.[5, 8, 10, 13, 14, 18, 23-25] The remaining approaches entail piezoelectrics,[21] MALDI TOF MS (matrix-assisted laser desorption/ionization time-of-flight mass spectrometry),[22] or various electrochemical techniques.[4, 6, 7, 9, 11, 12, 15-17, 19, 20] Of those schemes based on electrochemical detection, only one employs simple and inexpensive constant potential amperometry, yet Pt nanoparticle labels are required.[17] Ideally, an amplification-free NA sensor would involve just the selective oligonucleotide probe and eliminate the need for additional reagents, labels or complicated signal transduction technologies; however the literature analysis presented above suggests that sensing schemes that meet this ideal are rare.

Although distinctly different than our technology, nanopore-based, resistive-pulse sensors have shown promise for both NA sequencing and detection of NAs of specific sequence.[26-32] First generation nanopore sensing was based on protein pores, such as modified αHL or MspA, inserted in lipid bilayers.[28, 29] However, these biological nanopores are unstable, exhibit limited design

[a] Chemical and Biomolecular Engineering Department, University of California, Los Angeles, Los Angeles, CA 90095, USA. E-mail: hmonbouq@ucla.edu; Fax: +1 310 206 4107; Tel: +1 310 825 8946
[b] Bioengineering Department, University of California, Los Angeles, Los Angeles, CA 90095
† B. Koo and A.M. Yorita are co-first authors, and their current addresses are Food and Drug Administration, Silver Spring, MD, United States; and Lawrence Livermore National Laboratory, Livermore, CA, United States, respectively.
Electronic Supplementary Information (ESI) available: See DOI: 10.1039/x0xx00000x

flexibility, and require carefully controlled environments.[33-36] Compared to biological nanopores, solid-state nanopores offer improved stability and design freedom in both pore geometry and surface chemistry,[37, 38] and have led to impressive commercial sequencing devices. However, nanopore-based DNA sequencing is complicated; it requires sophisticated electronics to distinguish current pulses in the pA and microsecond regimes and complex decoding since the measured current pulses typically result from a combination of multiple nucleotides in the pore.[33-36] Also, the detection of a pathogen in body fluid, for example, does not necessarily require the sequencing of NA. Rather, the detection of NA of particular sequence most often is sufficient to determine the presence of a pathogen in a sample. Here again, the small size of biological nanopores has been exploited to detect the presence of target NA sequences since double-stranded probe-target hybrids cannot fully traverse αHL or MspA and this causes longer-lived pore blockages of ~150 microseconds or more during the unzipping of the probe-target hybrid.[39] Through this approach, the measurement bandwidth required is decreased and miRNA has been detected at levels down to 100 fM.[32] Nevertheless, this technology still requires relatively sophisticated electronics.

Previously, we introduced a concept for a pore-based device based on a drawn pipette tip（2 μm in diameter）as the "micropore". Rather than sensing a resistive-pulse, it entails the straightforward detection of a sustained pore blockage event that manifests as a step-change in ionic current, which can be measured with inexpensive electronics. In order to capture target NA, polystyrene beads (3 μm in diameter) were conjugated with uncharged peptide nucleic acid (PNA) as sequence-specific probes.[40-44] Upon binding target NA, the bead conjugates become charged and mobile in an electric field. When the bead conjugates with hybridized target approach the pore opening, the ionic current through the pore is restricted, which results in a sustained step change in current that signals the presence of the target NA. Importantly, the strong electric field at the pore mouth removes nonspecifically bound NA. Thus, this sensor could distinguish between complementary and non-complementary NA sequences, and no false positives were observed with both 1613-base DNA oligomers and 16S rRNA as targets at 10 fM.[40-42]

Reflection on these promising results suggested that scaling the pore and bead sizes into the nano-regime should enable improved performance and lower limits of detection. The equation below shows the relationship between the mobility, m, and the radius, r_p, of a charged particle in an aqueous solution of low ionic strength in a uniform electric field, E,

$$m = \frac{v_E}{E} = \frac{q}{6\pi\mu r_p}$$

where v_E is the drift velocity, q is the charge on the particle, and μ is the viscosity of the fluid. Since mobility is inversely proportional to the particle size, smaller beads are expected to have greater mobility when just a few target NAs are hybridized to bead-PNA conjugates. This implies that lower limits of detection may be achieved by decreasing the size of beads and corresponding pores.

Motivated by this analysis, we have developed the means to fabricate thin glass membranes in which a nanopore may be milled with a focused ion beam (FIB). By replacing the drawn glass pipette tip with a glass nanopore, the pore and bead size can be decreased. To test the ability of our device to detect NAs from actual organisms, we sought to detect specific 16S rRNA sequences. The sensing of 16S rRNA is attractive for detection of bacterial pathogens; because its sequence is species-specific, and 16S rRNA is present at ~10,000 copies per viable cell.[45, 46] The model target organism used in our work described here is a non-pathogenic strain of *E. coli* (ATCC 25922) with well-characterized oligonucleotide probes for its 16S rRNA.[47, 48]

Materials and methods

Polystyrene microbeads of 820 nm diameter and carboxylic acid surface functionality as well as Vivaspin® 2 mL ultrafiltration devices were purchased from Bangs Laboratories, Inc. (Fishers, IN). Methoxypolyethylene glycol amine (MW 750), gold etchant, and ethanolamine were obtained from Sigma-Aldrich (St. Louis, MO). Peptide nucleic acid (PNA) probe sequences were purchased from PNA Bio (Thousand Oaks, CA), and arrived as >95% HPLC-purified, lyophilized powders. The target PNA probe sequence for detecting *E. coli* (ATCC 25922) 16S rRNA was NH_2-$(CH_2CH_2OCH_2CH_2OCH_2CO)_6$-CTC CTT CCC TCA TTT CA.[46] The positive control PNA probe sequence to detect the 16S rRNA of both *E. coli* and *P. putida* was NH_2-$(CH_2CH_2OCH_2CH_2OCH_2CO)_6$-CTG CCT CCC GTA GGA.[49] *E. coli* (ATCC 25922), *P. putida* (ATCC 12633), soy broth and nutrient broth were purchased from American Type Culture Collection (Manassas VA). The RNeasy Protect Bacteria Mini Kit was purchased from Qiagen Sciences Inc. (Germantown, MD). Four-inch borosilicate glass wafers were obtained from Plan Optik (Elsoff, Germany) and photoresist (AZ®-5214 E) was purchased from AZ Electronic Materials (Luxembourg). Buffered oxide etchant (BOE), hydrofluoric acid (49%), hydrochloric acid (37%), and chromium etchant (CR–7S) were supplied by KMG Electronic Chemicals (Houston, TX). Potassium hydroxide (KOH) and J.T.Baker® ALEG™-380LM were purchased from Avantor Performance Materials (Center Valley, PA). Blue tape was obtained from Semiconductor Equipment Corporation (Moonpark, CA). Two mm-diameter, 4 mm-long Ag/AgCl pellet electrodes were purchased from A-M Systems, Inc. (Carlsborg, WA). GE Healthcare Life Sciences Anotop 25 syringe filters (25 mm-diameter, 0.02 μm pore) were supplied by Genesee Scientific (San Diego, CA).

Teflon chambers measuring 6 mm × 6 mm × 8 mm were custom-machined from Teflon blocks by the UCLA HSSEAS R & D Shops. A 4 mm-diameter hole was bored into the side of each chamber to create an opening to the glass chip, which was sandwiched between two Teflon chambers (see below).

Fabrication of Nanopores in Glass Membranes

Four inch-diameter glass borosilicate wafers (200 μm thick) were first patterned with a mask consisting of titanium, gold, and photoresist. Titanium (20 nm thick) and gold (200 nm thick) were

deposited from evaporated metal, and the photoresist was spin-coated on top and patterned. The gold and titanium were etched by gold etchant and buffered oxide etchant (BOE) in sequence. The resulting pattern exposed areas of the glass wafer that outline each glass chip via perforations in the glass, as well as the areas that are etched to create the glass membranes. The wafer was then immersed in a mixture of hydrofluoric acid (HF) and hydrochloric acid (HCl) (HF (49%) : HCl (37%) : DI water = 10 : 1 : 11) to obtain smooth surfaces. The backside of the wafer was protected by blue tape, to prevent any etching of the glass on the back of the wafer. The etch depth was monitored using a profilometer to track membrane thickness. Once the desired membrane thickness was achieved, the mask was removed using ALEG^{TM}-380LM photoresist stripper, gold etchant, and BOE. Twenty nm of chromium was then deposited via evaporation so that SEM could be used with the focused ion beam (FIB) for the pore milling process. A nanopore was milled at the center of the etched membrane using the FIB instrument (FEI Nova 600 Nanolab DualBeam SEM/FIB). Finally, the chromium layer was removed with chromium etchant, and the wafer was diced into 64 separate chips, each 1 cm × 1 cm in dimension. Figure 1 shows images of a fabricated chip with a nanopore at the center of the membrane. The pore is tapered somewhat with the larger diameter end on the etched side of the glass chip and the smaller opening on the smooth backside.

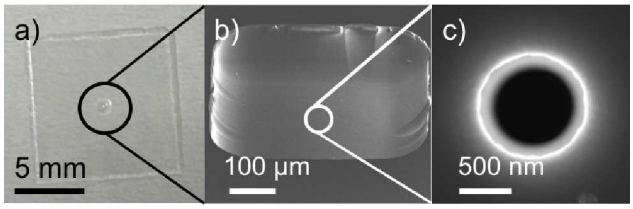

Fig. 1 a) A micromachined 1 cm × 1 cm glass chip. b) A SEM image of an etched membrane. (angled view), c) A SEM image of a glass nanopore milled using FIB.

Coupling PNA Probes to Microspheres

One µL of 820-nm-diameter, carboxylic group-functionalized polystyrene microspheres at a concentration of 3.25 × 10^{11}/mL were washed three times with MES buffer (100 mM 2-(N-morpholino)ethanesulfonic acid, pH 4.5). Upon re-suspension of the beads in each wash, the microspheres were centrifuged at 14,000 rpm for 15 minutes. After the third wash, the beads were re-suspended in 0.6 mL MES buffer, to which 1-[3-(dimethylamine) propyl]-3-ethylcarbodiimide (EDC) was added at a final concentration of 200 mM. This solution was incubated at 50 °C for 15 minutes. Next, 1.14 nmoles of the PNA target probe or universal probe were added to the buffer. This amount of PNA was optimized and estimated to correspond to about a 10^{14} PNA/cm^2 surface coverage of the beads. Due to the amine group at the end of each PNA oligonucleotide, EDC-based coupling reactions occur with the carboxylic groups on the beads to covalently bond PNA to beads. The reaction mixture was allowed to incubate for two hours at 50 °C. Next, methoxypolyethylene glycol amine (mPEG-amine) was added to a final concentration of 100 mM in the coupling solution and incubated for one hour at 50 °C. Addition of the mPEG-amine was included to inhibit bead aggregation and to reduce bead interactions with the glass chip surfaces.[50] Finally, 138 mM ethanolamine was added to the solution to fully cap any remaining carboxylic groups on the beads, thus ensuring that the bead conjugates were essentially charge neutral. This reaction mixture was incubated for an additional hour at 50 °C. The beads were then washed three times in 0.4× SSC buffer, consisting of 60 mM NaCl, 6 mM trisodium citrate, and 0.1% Triton X-100, pH 8. Beads were stored in the testing buffer, consisting of 10 mM KCl, 5.5 mM HEPES, and 0.01% Tween-80, pH 7. A portion of the beads was removed for zeta potential measurement to verify near-neutral effective charge of the bead surfaces and to confirm successful capping of carboxylic groups on the beads. The zeta potential was measured with the beads suspended in the testing buffer, using a Malvern Zetasizer Nano ZS (Malvern Instruments Ltd, Worchestershire, England).

Bacterial Culturing and Counting

ATCC Tryptic soy broth (15 g in 500 mL water) was made for culturing *E. coli*, ATCC 25922. ATCC Nutrient broth (4 g in 500 mL water) was made for culturing *P. putida*, ATCC 12633. Both broths were sterilized at 121 °C for 20 minutes. Since both bacterial strains arrived as lyophilized powders, cultures were initiated by mixing the bacterial preparations in 3 mL of broth. The *E. coli* culture was incubated at 37 °C at 250 rpm overnight. The *P. putida* culture was incubated at 26 °C at 250 rpm overnight. These cultures were mixed with 13% glycerin and frozen at -80 °C to serve as starter cultures. To prepare cultures for RNA extraction, 3 mL of tryptic soy broth was mixed with a small amount of the frozen *E. coli* culture prepared as described above. This culture was incubated at 37 °C at 250 rpm overnight. Similarly, 3 mL of nutrient broth was mixed with frozen *P. putida* culture and incubated at 26 °C at 250 rpm overnight. After reaching log phase, cells from both bacterial cultures were serially diluted, plated and incubated overnight prior to performing colony counts.

RNA Extraction

For work to determine the detection limit for *E. coli* 16S rRNA (Case I, Fig. 2), the total RNA of both *E. coli* and *P. putida* were separately extracted from pure cultures. A Qiagen RNeasy Protect Bacteria Mini Prep Kit was used for total RNA extraction and purification. Each extraction began with 1.7 mL of bacterial culture, and total extracted RNA was eluted into 100 µL of RNase-free purified water. The RNA concentration was measured using a Thermo Scientific Nanodrop 2000. Based on previous work regarding the percentage of 16S rRNA in total RNA for *E. coli* and *P. putida*,[42] the concentration of 16S rRNA in the samples of extracted RNA from *E. coli* and *P. putida* were estimated to be 75.7 nM and 100.7 nM, respectively. Subsequently, the eluted RNA solution was serially diluted to achieve target concentrations for hybridization and subsequent detection studies.

In preparation for work to verify the detection of viable *E. coli* against a background of *P. putida*, 10 CFU/mL of *E. coli* and 10^6

CFU/mL of *P. putida* were mixed prior to RNA extraction as described above (Case II, Fig. 2). The viable bacterial concentrations (CFU/mL) were determined by serial dilution and colony counts, as described above.

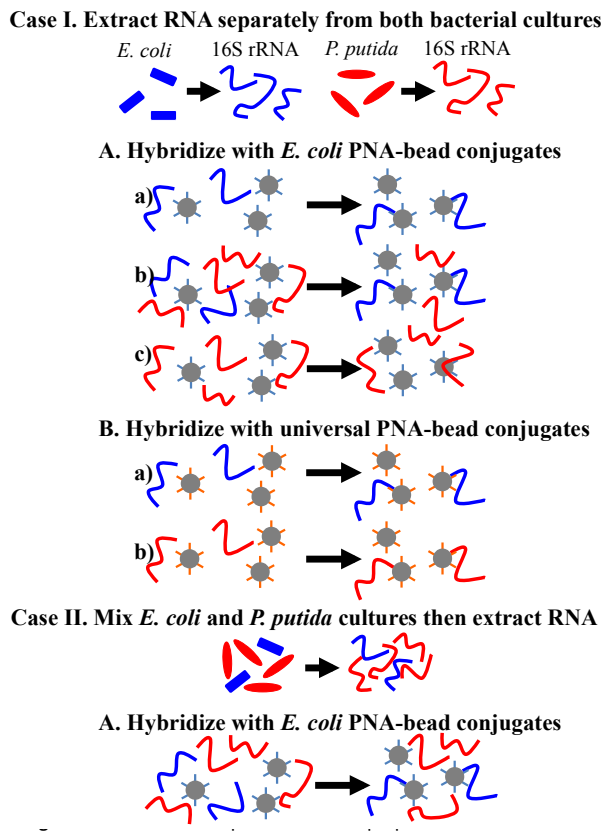

RNA was extracted separately from *E. coli* and *P. putida* cultures. *E. coli* RNA was diluted serially to assay for limit of detection with PNA-bead conjugates selective for *E. coli* 16S rRNA (I-A-a). *E. coli* RNA was mixed with 10^6-fold more *P. putida* RNA and hybridized to *E. coli* PNA-bead conjugates to test for interference (I-A-b). *P. putida* RNA was hybridized to *E. coli* PNA-bead conjugates (negative control, I-A-c). *E. coli* and *P. putida* RNA was separately hybridized with universal PNA-bead conjugates (positive controls, I-B-a and I-B-b). Case II. *E. coli* and *P. putida* cultures were mixed to give preparations of known CFU/mL of each species, then RNA was extracted and hybridized with *E. coli* PNA-bead conjugates (II-A).

Hybridization of RNA to PNA-Bead Conjugates

Beads with conjugated PNA probes were washed three times with 0.4× SSC buffer and once with hybridization buffer (10 mM NaCl, 25 mM Tris-HCl, pH 7). Aliquots from the RNA preparations were added to achieve the desired concentration combined with approximately 1.26 × 10^6 PNA-bead conjugates in 600 µL of hybridization buffer. For Case I-A, RNA samples were hybridized with beads conjugated to PNA selective for *E. coli* only (*E. coli* PNA-beads). *E. coli* RNA was added at decreasing concentration to determine the *E. coli* 16S rRNA detection limit (Case I-A-a). For Case I-A-b, *E. coli* RNA (1 aM 16S rRNA) was mixed with that of *P. putida* at 1 pM to assess selectivity; and 1 pM *P. putida* was used in a negative control to ensure that no current signal was detected in absence of the target *E. coli* 16S rRNA (Case I-A-c). For case I-B, diluted RNA from both *E. coli* and *P. putida* was separately mixed with beads conjugated with the universal PNA probe, complementary to both *E. coli* and *P. putida* 16S rRNA, to serve as a positive control. For case II-A, extracted RNA samples from mixed bacterial cultures (10 CFU/mL of *E. coli* and 10^6 CFU/mL of *P. putida*) were hybridized to bead conjugates with PNA probe specific for *E. coli*. In all cases, hybridization was conducted overnight at room temperature on a rotator.

System Setup and Detection Process

After overnight hybridization, each bead solution was cleaned with Vivaspin® 2 mL ultrafiltration devices using a centrifuge run at 700 rpm for 5 minutes. These centrifuge filters were used to minimize bead loss during washing steps. The beads were cleaned once in 0.4× SSC buffer and once more in testing buffer (10 mM KCl, 5.5 mM HEPES, 0.01% Tween-80, pH 7). Finally, the beads were suspended in 200 µL testing buffer and sonicated at 50 °C for 5 min. Sonication in warm solution helps to remove non-specifically bound RNA since melting temperatures of PNA-nucleic acid duplexes drops significantly even with a single mismatch.[51]

A glass chip containing a single nanopore was sandwiched between two Teflon chambers (each measuring 6 mm × 6 mm × 8 mm, 216 µL) using polydimethylsiloxane (PDMS) o-rings as seals. Test buffer (200 µL) was pipetted into each chamber to ensure that the pore connecting the two chambers was filled with buffer. One Ag/AgCl pellet electrode was placed in each of the chambers on either side of the pore. These electrodes were connected to a multichannel potentiostat (VMP3) interfaced to a computer running EC-Lab software for data collection (Bio-Logic USA, LLC, Knoxville, TN). Beads (approximately 5 × 10^5) were injected in the chamber on the smooth backside of the chip where the tapered pore opening is smallest, since fewer permanent blocks (see below) and shorter response times were observed in this case. After bead addition, the current was monitored for sustained ionic current drops at 1.5 V that would signal detection of target 16S rRNA. After a current drop was seen due to pore blockage, the potential was held for at least one minute to ensure that the block was not simply a transient caused by PNA-bead conjugates weakly bound to non-target RNA. If the current drop persisted for a minute or less, we referred to it as a "transient block", not indicative of a target rRNA detection event. If no blocks were observed after an hour or more of monitoring, it was considered to be a negative detector response. After each confirmed block (positive detector response), the polarity of the field was reversed to -1.5 V to attempt to unblock the pore.

Results and discussion

Results of pore blocking experiments are shown in Tables 1-3 and Figure 3. For Case I-A-a (Table 1), the detection limit of the system was determined by incubating *E. coli* PNA-beads with decreasing concentrations of isolated *E. coli* RNA. Beads hybridized with the

16S rRNA of target *E. coli* at 1 pM to 1 aM were successfully detected using our glass nanopores with no false negatives, indicating that the limit of detection (LOD) of this device is ≤1 aM. Compared to the 10 fM LOD of our previous device based on a drawn glass pipette, the new ≤1 aM LOD constitutes an improvement of at least 4 orders of magnitude.[42] This result is in agreement with our hypothesis that the LOD would decrease with decreasing bead size, possibly due to increased bead mobility, but we cannot rule out the possibility that the lower LOD is primarily the result of the changed glass pore geometry. Nevertheless, a 1 aM LOD is competitive with state-of-the-art nucleic acid detection schemes, including those based on NA amplification, with published LODs of sub-femtomolar to hundreds of zeptomolar.[4-25, 52-57] Even though a LOD of 1 aM is not the lowest on record, other NA amplification-free techniques with lower reported LODs require labels and/or more complex technology as described in the Introduction.

Table 1 Summary of results where *E. coli* PNA-beads are hybridized separately to *E. coli* RNA (Case I-A-a) and to *P. putida* RNA (negative control, Case I-A-c).

	Target *E. coli* (Case I-A-a)		Control *P. putida* (Case I-A-c)		
Concentration		Drop/Reversible	Concentration		Drop/Reversible
1 pM	Expt. 1	Yes/R	1 pM	Expt. 1	No*
	Expt. 2	Yes/R		Expt. 2	No
	Expt. 3	Yes/R		Expt. 3	No
100 fM	Expt. 1	Yes/R			
10 fM	Expt. 1	Yes/R			
	Expt. 2	Yes/R			
	Expt. 3	Yes/R			
1 fM	Expt. 1	Yes/R			
	Expt. 2	Yes/R			
100 aM	Expt. 1	Yes/R			
	Expt. 2	Yes/N			
10 aM	Expt. 1	Yes/R			
1 aM	Expt. 1	Yes/N*			
	Expt. 2	Yes/R			
	Expt. 3	Yes/R			

Yes: permanent block was observed without transient block, No: neither permanent block nor transient block was observed, No*: transient block was observed, R: open current returned to the original level after a detection event and a reverse in voltage polarity, N*: open current returned to the original level but no subsequent detection events observed. N: open current did not return to the original level.

The LOD of 1 aM with our device also is remarkable since the order-of-magnitude average number of target 16S rRNA molecules per bead is estimated at 0.0001, which corresponds to ~10 beads with one bound RNA (using Poisson statistics, see Supporting Information) in the measurement volume. Thus, it appears that just one bound target RNA molecule per bead for an exceedingly small fraction of the bead population (total ~10^6 beads) is sufficient to give a reproducible detection event.

Table 2 Summary of positive control results where universal PNA-bead conjugates are hybridized separately to *E. coli* RNA (Case I-B-a) and to *P. putida* RNA (Case I-B-c).

		Target *E. coli* (Case I-B-a)	Control *P. putida* (Case I-B-c)
Concentration		Drop/Reversibility	Drop/Reversibility
100 aM	Expt. 1	Yes/N	Yes/N
10 aM	Expt. 1	Yes*/R	Yes/N
1 aM	Expt. 1	Yes/N	Yes/R
	Expt. 2	Yes/R	Yes/R
	Expt. 3	Yes/N	Yes*/N

Yes: permanent block was observed without transient block, No: neither permanent block nor transient block was observed, Yes*: transient block was observed followed by a detection event, R: open current returned to the original level after a detection event and a reverse in voltage polarity, N: open current did not return to the original level.

As evidence of selectivity, test runs with a high concentration (1 pM) of *P. putida* RNA (negative control, Case I-A-c) hybridized with beads presenting PNA selective for *E. coli* 16S rRNA, resulted in no false positives (Table 1). One transient block was observed in one out of three experimental runs, however these transient events of less than 1 min were not taken as positive signals. As we have hypothesized in the past,[40-42] the transient blockages may be due to non-target RNA bound weakly to the PNA-bead conjugates, which is stripped away easily by the strong electric field at the pore opening. Subsequently, the bead becomes near neutral in charge and is removed from the glass nanopore by the opposing electroosmotic flow.

Table 3 Summary of results when RNA of *E. coli* is mixed with *P. putida* RNA and hybridized with *E. coli* PNA-beads (Case I-A-b); and when RNA extracted from mixtures of cultures of *E. coli* and *P. putida* and hybridized with *E. coli* PNA-beads (Case II-A).

1 aM *E. coli* + 1 pM *P. putida* (Case I-A-b)		10 CFU/mL *E. coli* + 10^6 CFU/mL *P. putida* (Case II-A)	
	Drop/Reversible		Drop/Reversible
Expt. 1	Yes/N	Expt. 1	Yes/R
Expt. 2	Yes/R	Expt. 2	Yes/R
Expt. 3	Yes/N	Expt. 3	Yes/R

Yes: permanent block was observed without transient block, R: open current returned to the original level after a detection event and a reverse in voltage polarity, N: open current did not return to the original level.

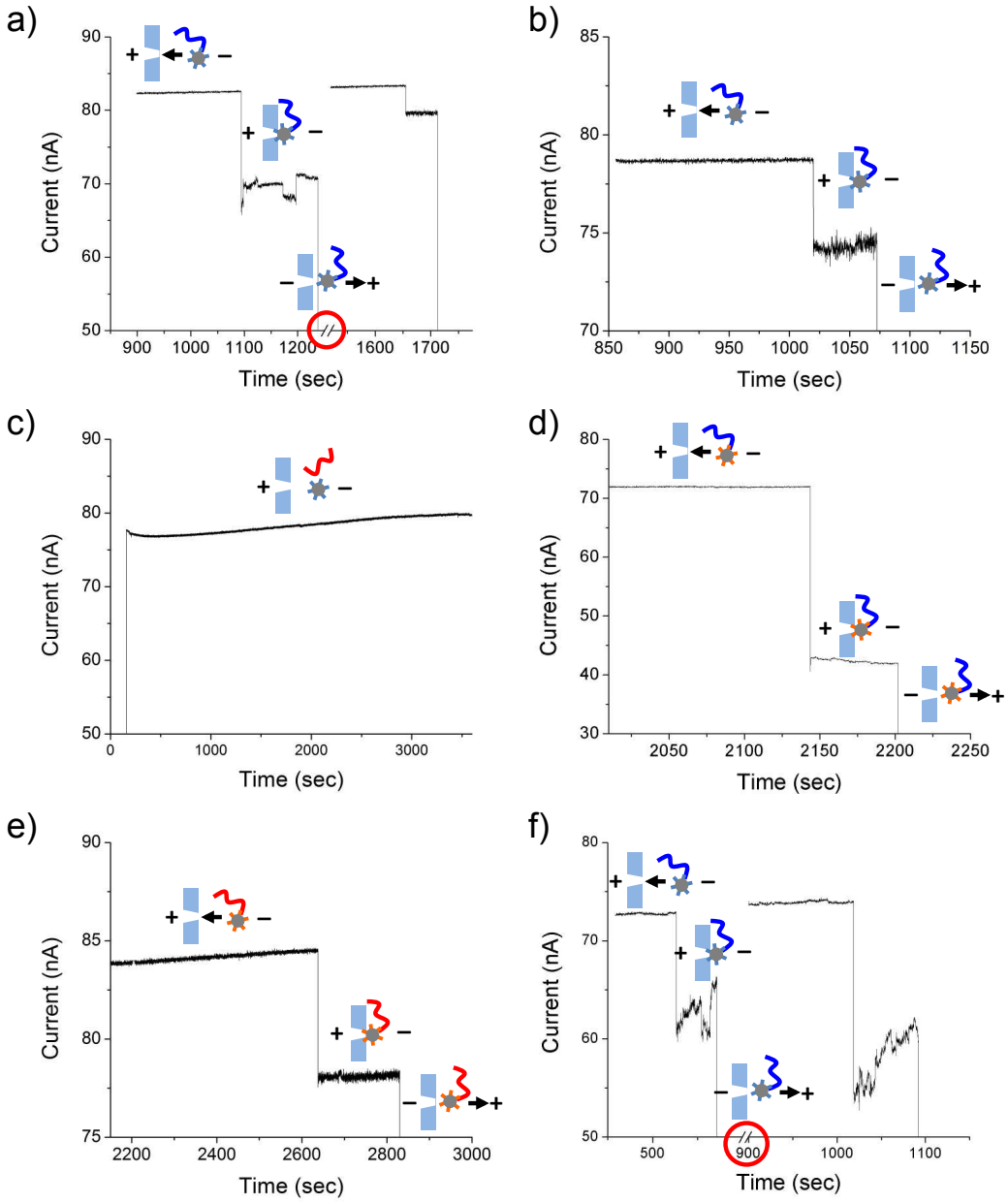

Fig. 3 Device current data with respect to time showing blockage events, or lack thereof during control runs. a) Case Ⅰ-A-a: *E. coli* PNA-beads hybridized with 1 aM *E. coli* 16S rRNA. b) Case Ⅰ-A-b: *E. coli* PNA-beads hybridized with 1 aM *E. coli* 16S rRNA in the presence of 1 pM *P. putida* RNA. c) Case Ⅰ-A-c: *E. coli* PNA-beads hybridized with 1 pM 16S rRNA of *P. putida* (negative control). d) Case Ⅰ-B-a: universal PNA-beads hybridized with 1 aM *E. coli* 16S rRNA (positive control). e) Case Ⅰ-B-b: universal PNA-beads hybridized with 1 aM *P. putida* 16S rRNA (positive control). f) Case II-A: *E. coli* PNA-beads hybridized with RNA extracted from a mixture of 10 *E. coli* CFU/mL and 10^6 *P. putida* CFU/mL.

One interesting point is that the reversibility of pore-blocking runs was always observed at target RNA concentrations higher than 100 aM (Tables 1-3). Reversibility is defined here as the recoverability of the open current observed prior to the first pore blockage by temporarily reversing the voltage polarity. Reversibility is taken as an indication that a pore blockage is due to a bead conjugate with hybridized target RNA held at the pore opening in a non-covalent manner. However, a significant number of runs at ≤100 aM were non-reversible for all PNA-bead conjugates and target RNA preparations as indicated by an "N" in Tables 1-3, which suggests that the electrostatic force acting on one or more beads at the pore mouth during a voltage reversal was insufficient to overcome the forces retaining the beads in place. The motion of a bead in the vicinity of the pore results primarily from the balance between the electrostatic force due to the negative charge on beads with hybridized RNA and the opposing drag force arising from

the electroosmotic flow through the pore.[58, 59] Since there are few beads with 2 or more hybridized target *E. coli* 16S rRNA at ≤100 aM, and non-reversibility was observed only at or below this concentration level, a possible implication is that the reduced electrostatic force on beads with lower charge (from only 1 bound NA) is insufficient to remove beads from the vicinity of the pore mouth. Adsorption of the less charged bead conjugates on the glass surface and/or ionic current rectification[60-62] may play a role. More study is needed to resolve this issue, although it does not detract from the analytical value of the device, since no false positives are observed.

Tests were also conducted using the universal PNA probe (Case I-B-a and I-B-b), to which it was expected that 16S rRNA from both bacterial species would hybridize and cause a current drop signal. As seen in Table 2, permanent blocks were observed down to 1 aM of 16S rRNA from either organism as expected, thus confirming the efficacy of our nanopore devices in detecting 16S rRNA from either *E. coli* or *P. putida* provided that complementary PNA is conjugated to the beads.

Case I-A-b was designed for the more realistic situation where RNA from *E. coli* and a 10^6-fold higher concentration of *P. putida* RNA were combined and incubated with PNA-beads. This test determines if detection of *E. coli* 16S rRNA is still attained at a very low LOD against a high background of off-target bacterial RNA. Consistent with the results of I-A-a, successful detection of 1 aM target *E. coli* 16S rRNA against this background was accomplished without false negatives (Table 3). The ability of our sensor to pick out target 16S rRNA in the presence of a million-fold greater concentration of off-target RNA, suggests that it could be used in an application in which other bacterial species may be present, such as in body fluids, drinking water, or food.

The Case I tests were conducted using RNA preparations from both bacteria with 16S rRNA concentration estimated from serial dilution of stock RNA extracts of measured concentration. In more realistic sample preparations, however, RNA could be lost, especially at the RNA extraction step, which could lead to false negatives despite the existence of target bacteria in actual samples. In order to address this situation (Case II-A), *E. coli* PNA-bead conjugates were hybridized to RNA extracted from mixed bacterial preparations consisting of 10 CFU/mL *E. coli* and 10^6 CFU/mL *P. putida*. A 10 CFU/mL *E. coli* concentration was chosen to ensure the strong likelihood that at least one viable target *E. coli* cell would be present in a ~1 mL sample taken from the mixed culture preparation. In all Case II-A runs, 16S rRNA of the target *E. coli* was successfully detected (Table 3). These results were expected since 10 CFU/mL *E. coli* corresponds to ~100 aM 16S rRNA (given ~10,000 rRNA copies per cell), which is much higher than the ≤1 aM limit of detection established with the Case I studies.

On the basis of the low LOD exhibited, the detection of pathogens using our device potentially could be extended to such real samples as body fluids, food, or dairy products. For example, commercial, nucleic acid amplification-based tests for gonorrhea have typical LODs in the ~10 CFU/mL range. Also, 10^5 CFU/mL is the standard for urinary tract infections;[49, 63, 64] 20 CFU/g for *E. coli* is the upper limit for satisfactory food quality;[65] and 10^4 CFU/g of *Staphylococcus aureus* or 10^6 CFU/g of *Bacillus cereus* serve as the standards for dairy products.[66]

Conclusions

Glass chips with a submicron-thick membrane and a single nanopore were microfabricated by a novel wet-etching method for detection of nucleic acids of specific sequence. Using these chips and our previously described signal transduction mechanism,[40-42] *E. coli* 16S rRNA was detected at 1 aM against a 10^6-fold background of *P. putida* RNA. This result constitutes a 10^4-fold improvement over our previous work with a first-generation microscale device, indicating that scaling to the nano-regime leads to the expected decrease in detection limit. Our RNA sensing device reproducibly detected a target sequence specific to *E. coli* 16S rRNA, and no false positives were observed in the presence of *P. putida* RNA but absence of *E. coli* RNA. Because this detection method uses simple electronics and has minimal reagent requirements, there is potential to develop a device that can quickly and inexpensively detect the presence of bacterial pathogens in body fluids, food and water.

Acknowledgements

This research was supported by NSF CBET (1265061).

References

1. H. Jayamohan, H. J. Sant and B. K. Gale, *Methods Mol. Biol. (N. Y., NY, U. S.)*, 2013, **949**, 305-334.
2. K. E. Templeton, S. A. Scheltinga, M. F. C. Beersma, A. C. M. Kroes and E. C. J. Claas, *J Clin Microbiol*, 2004, **42**, 1564-1569.
3. D. Whitcombe, J. Theaker, S. P. Guy, T. Brown and S. Little, *Nature Biotechnology*, 1999, **17**, 804-807.
4. C. P. Chen, A. Ganguly, C. Y. Lu, T. Y. Chen, C. C. Kuo, R. S. Chen, W. H. Tu, W. B. Fischer, K. H. Chen and L. C. Chen, *Anal Chem*, 2011, **83**, 1938-1943.
5. R. D'Agata, G. Breveglieri, L. M. Zanoli, M. Borgatti, G. Spoto and R. Gambari, *Anal Chem*, 2011, **83**, 8711-8717.
6. H. Dong, Z. Zhu, H. Ju and F. Yan, *Biosens Bioelectron*, 2012, **33**, 228-232.
7. W. Gao, H. Dong, J. Lei, H. Ji and H. Ju, *Chem Commun (Camb)*, 2011, **47**, 5220-5222.
8. J. Hu, P. C. Zheng, J. H. Jiang, G. L. Shen, R. Q. Yu and G. K. Liu, *Analyst*, 2010, **135**, 1084-1089.
9. Q. Hu, W. Hu, J. Kong and X. Zhang, *Microchimica Acta*, 2014, **182**, 427-434.
10. G. Y. Kim and A. Son, *Anal Chim Acta*, 2010, **677**, 90-96.
11. Y. J. Kim, J. E. Jones, H. Li, H. Yampara-Iquise, G. Zheng, C. A. Carson, M. Cooperstock, M. Sherman and Q. Yu, *Journal of Electroanalytical Chemistry*, 2013, **702**, 72-78.
12. C. Li, D. Wu, X. Hu, Y. Xiang, Y. Shu and G. Li, *Anal Chem*, 2016, **88**, 7583-7590.
13. G. Li, L. Zhu, Z. Wu, Y. He, H. Tan and S. Sun, *Anal Chem*, 2016, **88**, 10994-11000.
14. W. Ma, H. Kuang, L. Xu, L. Ding, C. Xu, L. Wang and N. A. Kotov, *Nat Commun*, 2013, **4**, 2689.

15. P. Ramnani, Y. Gao, M. Ozsoz and A. Mulchandani, *Anal Chem*, 2013, **85**, 8061-8064.
16. P. Sahoo, S. Suresh, S. Dhara, G. Saini, S. Rangarajan and A. K. Tyagi, *Biosens Bioelectron*, 2013, **44**, 164-170.
17. E. Spain, H. McArdle, T. E. Keyes and R. J. Forster, *Analyst*, 2013, **138**, 4340-4344.
18. V. Srinivasan, A. K. Manne, S. G. Patnaik and S. S. Ramamurthy, *ACS Appl Mater Interfaces*, 2016, **8**, 23281-23288.
19. S. Tripathy, S. R. Krishna Vanjari, V. Singh, S. Swaminathan and S. G. Singh, *Biosens Bioelectron*, 2017, **90**, 378-387.
20. T. Widaningrum, E. Widyastuti, F. W. Pratiwi, A. I. Faidoh Fatimah, P. Rijiravanich, M. Somasundrum and W. Surareungchai, *Talanta*, 2017, **167**, 14-20.
21. W. Wu, C. E. Kirimli, W. H. Shih and W. Y. Shih, *Biosens Bioelectron*, 2013, **43**, 391-399.
22. B. Yang, K. Gu, X. Sun, H. Huang, Y. Ding, F. Wang, G. Zhou and L. L. Huang, *Chem Commun (Camb)*, 2010, **46**, 8288-8290.
23. J. Zhou, Q. X. Wang and C. Y. Zhang, *J Am Chem Soc*, 2013, **135**, 2056-2059.
24. H. A. Ho, K. Dore, M. Boissinot, M. G. Bergeron, R. M. Tanguay, D. Boudreau and M. Leclerc, *J Am Chem Soc*, 2005, **127**, 12673-12676.
25. J. M. Nam, S. I. Stoeva and C. A. Mirkin, *J Am Chem Soc*, 2004, **126**, 5932-5933.
26. V. S. K. Balagurusamy, P. Weinger and X. S. Ling, *Nanotechnology*, 2010, **21**, 335102.
27. D. Fologea, M. Gershow, B. Ledden, D. S. McNabb, J. A. Golovchenko and J. L. Li, *Nano Lett*, 2005, **5**, 1905-1909.
28. S. Howorka, S. Cheley and H. Bayley, *Nature Biotechnology*, 2001, **19**, 636-639.
29. J. J. Kasianowicz, E. Brandin, D. Branton and D. W. Deamer, *P Natl Acad Sci USA*, 1996, **93**, 13770-13773.
30. R. F. Purnell and J. J. Schmidt, *Acs Nano*, 2009, **3**, 2533-2538.
31. O. A. Saleh and L. L. Sohn, *Nano Lett*, 2003, **3**, 37-38.
32. Y. Wang, D. L. Zheng, Q. L. Tan, M. X. Wang and L. Q. Gu, *Nat Nanotechnol*, 2011, **6**, 668-674.
33. M. Akeson, D. Branton, J. J. Kasianowicz, E. Brandin and D. W. Deamer, *Biophys J*, 1999, **77**, 3227-3233.
34. S. Carson and M. Wanunu, *Nanotechnology*, 2015, **26**, 074004.
35. J. L. Li, M. Gershow, D. Stein, E. Brandin and J. A. Golovchenko, *Nature Materials*, 2003, **2**, 611-615.
36. A. Meller, L. Nivon, E. Brandin, J. Golovchenko and D. Branton, *P Natl Acad Sci USA*, 2000, **97**, 1079-1084.
37. C. Dekker, *Nat Nanotechnol*, 2007, **2**, 209-215.
38. A. J. Storm, J. H. Chen, X. S. Ling, H. W. Zandbergen and C. Dekker, *Nature Materials*, 2003, **2**, 537-540.
39. A. F. Sauer-Budge, J. A. Nyamwanda, D. K. Lubensky and D. Branton, *Phys Rev Lett*, 2003, **90**, 238101.
40. L. Esfandiari, M. Lorenzini, G. Kocharyan, H. G. Monbouquette and J. J. Schmidt, *Analytical Chemistry*, 2014, **86**, 9638-9643.
41. L. Esfandiari, H. G. Monbouquette and J. J. Schmidt, *J Am Chem Soc*, 2012, **134**, 15880-15886.
42. L. Esfandiari, S. Wang, S. Wang, A. Banda, M. Lorenzini, G. Kocharyan, H. G. Monbouquette and J. J. Schmidt, *Biosensors (Basel)*, 2016, **6**, 37.
43. O. Brandt and J. D. Hoheisel, *Trends in Biotechnology*, 2004, **22**, 617-622.
44. P. E. Nielsen, M. Egholm, R. H. Berg and O. Buchardt, *Science*, 1991, **254**, 1497-1500.
45. J. M. Janda and S. L. Abbott, *J Clin Microbiol*, 2007, **45**, 2761-2764.
46. H. Stender, A. J. Broomer, K. Oliveira, H. Perry-O'Keefe, J. J. Hyldig-Nielsen, A. Sage and J. Coull, *Appl Environ Microb*, 2001, **67**, 142-147.
47. B. M. Fuchs, G. Wallner, W. Beisker, I. Schwippl, W. Ludwig and R. Amann, *Appl Environ Microb*, 1998, **64**, 4973-4982.
48. B. P. Nelson, M. R. Liles, K. B. Frederick, R. M. Corn and R. M. Goodman, *Environ Microbiol*, 2002, **4**, 735-743.
49. C. P. Sun, J. C. Liao, Y. H. Zhang, V. Gau, M. Mastali, J. T. Babbitt, W. S. Grundfest, B. M. Churchill, E. R. B. McCabe and D. A. Haake, *Mol Genet Metab*, 2005, **84**, 90-99.
50. D. A. C. Thomson, K. Dimitrov and M. A. Cooper, *Analyst*, 2011, **136**, 1599-1607.
51. T. Ratilainen, A. Holmen, E. Tuite, P. E. Nielsen and B. Norden, *Biochemistry-Us*, 2000, **39**, 7781-7791.
52. M. A. Bangar, D. J. Shirale, H. J. Purohit, W. Chen, N. V. Myung and A. Mulchandani, *Electroanal*, 2011, **23**, 371-379.
53. H. D. Hill and C. A. Mirkin, *Nature Protocols*, 2006, **1**, 324-336.
54. Y. Q. Liu, M. Zhang, B. C. Yin and B. C. Ye, *Analytical Chemistry*, 2012, **84**, 5165-5169.
55. M. Rochelet-Dequaire, B. Limoges and P. Brossier, *Analyst*, 2006, **131**, 923-929.
56. F. Wei, J. H. Wang, W. Liao, B. G. Zimmermann, D. T. Wong and C. M. Ho, *Nucleic Acids Res*, 2008, **36**, e65.
57. X. L. Zuo, F. Xia, A. Patterson, H. T. Soh, Y. Xiao and K. W. Plaxco, *Chembiochem*, 2011, **12**, 2745-2747.
58. M. Firnkes, D. Pedone, J. Knezevic, M. Doblinger and U. Rant, *Nano Lett*, 2010, **10**, 2162-2167.
59. S. Lee, Y. H. Zhang, H. S. White, C. C. Harrell and C. R. Martin, *Analytical Chemistry*, 2004, **76**, 6108-6115.
60. M. L. Kovarik, K. M. Zhou and S. C. Jacobson, *J Phys Chem B*, 2009, **113**, 15960-15966.
61. Z. S. Siwy, *Advanced Functional Materials*, 2006, **16**, 735-746.
62. H. S. White and A. Bund, *Langmuir*, 2008, **24**, 2212-2218.
63. E. H. Kass, *Arch Intern Med*, 1957, **100**, 709-714.
64. G. Schmiemann, E. Kniehl, K. Gebhardt, M. M. Matejczyk and E. Hummers-Pradier, *Dtsch Arztebl Int*, 2010, **107**, 361-U369.
65. R. J. Gilbert, J. de Louvois, T. Donovan, C. Little, K. Nye, C. D. Ribeiro, J. Richards, D. Roberts and F. J. Bolton, *Commun Dis Public Health*, 2000, **3**, 163-167.
66. Compliance Policy Guide Sec. 527.300 Dairy Products-Microbial Contaminants and Alkaline Phosphatase Activity; Availability--A notice by the Food and Drug Administration on 12/23/2010. 2010, 80826-80827.

a

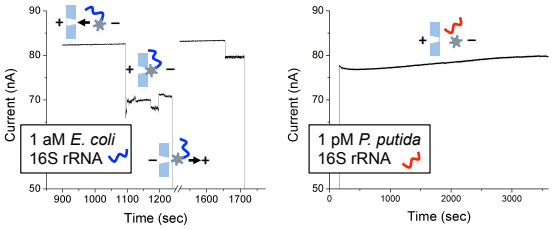

A novel means to detect bacteria based on PCR-free, optics-free sensing of 16S RNA at ultralow concentration (i.e., 10^{-18} M).